UVicSPACE: Research & Learning Repository

University of Victoria

Faculty of Engineering

Faculty Publications

This is a post-print version of the following article:

Assessment of self-healing and durability parameters of concretes incorporating crystalline admixtures and Portland Limestone Cement

Pejman Azarsa, Rishi Gupta, & Alireza Biparva

May 2019

The final publication is available via ScienceDirect at:

https://doi.org/10.1016/j.cemconcomp.2019.02.017

Citation for this paper:

Azarsa, P., Gupta R., & Biparva, A. (2019). Assessment of self-healing and durability parameters of concretes incorporating crystalline admixtures and Portland Limestone Cement. *Cement and Concrete Composites*, 99, 17-31. https://doi.org/10.1016/j.cemconcomp.2019.02.017.

Assessment of self-healing and durability parameters of concretes incorporating crystalline admixtures and Portland Limestone Cement

Pejman Azarsa[a], Rishi Gupta[a,*], Alireza Biparva[b]

[a] Facility for Innovative Materials and Infrastructure Monitoring (FIMIM), Department of Civil Engineering, University of Victoria, 3800 Finnerty Rd., Victoria, B.C., Canada

[b] Research and Development Manager, Kryton International Inc, 1645 East Kent Ave N, Vancouver, B.C., Canada

Highlights

- Chloride and water permeability tests are compared/correlated for concretes containing crystalline admixtures (CA).
- Influences of CA on the crack self-healing of concrete are studied based on permeability reduction of cracked specimens.
- Portland Limestone Cement (PLC) is slightly more effective than Ordinary Portland cement (OPC) in improving concrete's durability and strength.
- Influencing parameters on electrical resistivity of concrete treated with CA are investigated.

Abstract

The repair of concrete structures damaged by water or water borne chemicals is estimated to cost billions of dollars annually worldwide. However, the solutions that can make concrete structures more sustainable and durable, are limited. The use of crystalline admixtures (CA) has a potential of improving the durability and reducing permeability of concrete structures especially those exposed to corrosive environments. This paper presents various investigations on the influence of crystalline admixtures on the strength, self-healing, and durability characteristics of concretes with two different cement types (Ordinary Portland Cement [OPC] and Portland Limestone Cement [PLC]). Test methods include the rapid chloride permeability (RCP), surface/bulk electrical resistivity and water permeability tests, self-healing test, compressive strength test and salt ponding test. The results indicate that the water permeability coefficient decreased by 3 times whereas the self-healing ratio increased by a higher rate by adding crystalline admixtures into the concrete mix. This paper presents empirical equations to correlate resistivity, total charge passed, or water permeability with each other. Further, the correlation between the surface and bulk resistivity is strong and the evidence from self-healing test suggests faster sealing of crack widths up to 250 µm for CA treated specimens.

Keywords:

Crystalline Admixtures, Self-healing, Chloride Diffusivity, Electrical Resistivity, Water Permeability

* Corresponding author. Tel.: +1 (250) 721 7033
Address: University of Victoria, Department of Civil Engineering, Engineering and Computer Science (ECS) 314, 3800 Finnerty Road, Victoria BC V8P 5C2
Email address: guptar@uvic.ca (R. Gupta)

1. Introduction

Self-healing (SH) materials are innate in the human body from the day we are born and can be identified by blood clotting mechanisms, repairing of fractured bones and even the continuous rebirth of the skeleton cells which typically results in a full renovation of the skeleton [1]. Interestingly, concrete is also not exempt from this phenomenon and can naturally heal itself to a certain degree. When a crack occurs inside the matrix, concrete can autogenously seal the crack through four mechanisms including (1) formation of calcium carbonate ($CaCO_3$), (2) continued hydration upon moisture contact, (3) swelling of cement matrix, and (4) sedimentation of debris which eventually results in concrete gaining its certain mechanical or durability properties (Fig. 1) [2]. In young concrete, continued hydration is the dominant healing mechanism because of its fairly high content of un-hydrated cement particles whereas calcium carbonate formation becomes the main mechanism at later age [3–5]. In the past two decades, great number of research studies have been conducted to understand various aspects of intrinsic SH in concrete [3–16]. Due to limited crack width closure potential (~200-300 μm) and uncertainty of natural healing [8,14,17–19], the concept of Engineered Self-healing Concrete (EShC), by artificially triggering healing agents such as microencapsulated bacteria or crystalline admixtures, has been introduced and recently become a significant topic of interest . Use of EShC in structures could lead to a decreased deterioration rate, less repair demands, minimized costs and eventually extended ultimate service life [20]. Additionally, it allows *in-situ* self-repair with no external human involvement for inaccessible structures. Considering EShC's benefits, influences on structural serviceability and sustainably, several smart methodologies have been employed to design this type of concrete, including chemical encapsulation [21–23], expansive agents and mineral admixtures [24,25], shape memory materials [26-27], bacteria-based concrete [28–31], hollow fibers [32–41], and self-healing triggered by self-controlled tight microcracking [2,8,42–51].

One of the smart materials for fabrication of EShC is crystalline admixtures (CA) which is one of the types of permeability-reducing admixture (PRA) with hydrophilic nature that can react easily with water. Typically, CA consist of a proprietary mix of active chemicals, implanted in a carrier of cement and sand, reacting with tricalcium silicates (C_3S) in the concrete compounds as described by the American Concrete Institute (ACI) Committee 212 [52]; however, in the study of Sisomphon *et al.* [25], it is stated that calcium hydroxide (CH) is the reactive component. As a result of the chemical reaction described in Equation 1 and deposition of integrally bonded crystals into the hardened cement paste, pressure resistance of modified matrix increases as high as 14 bars [52].

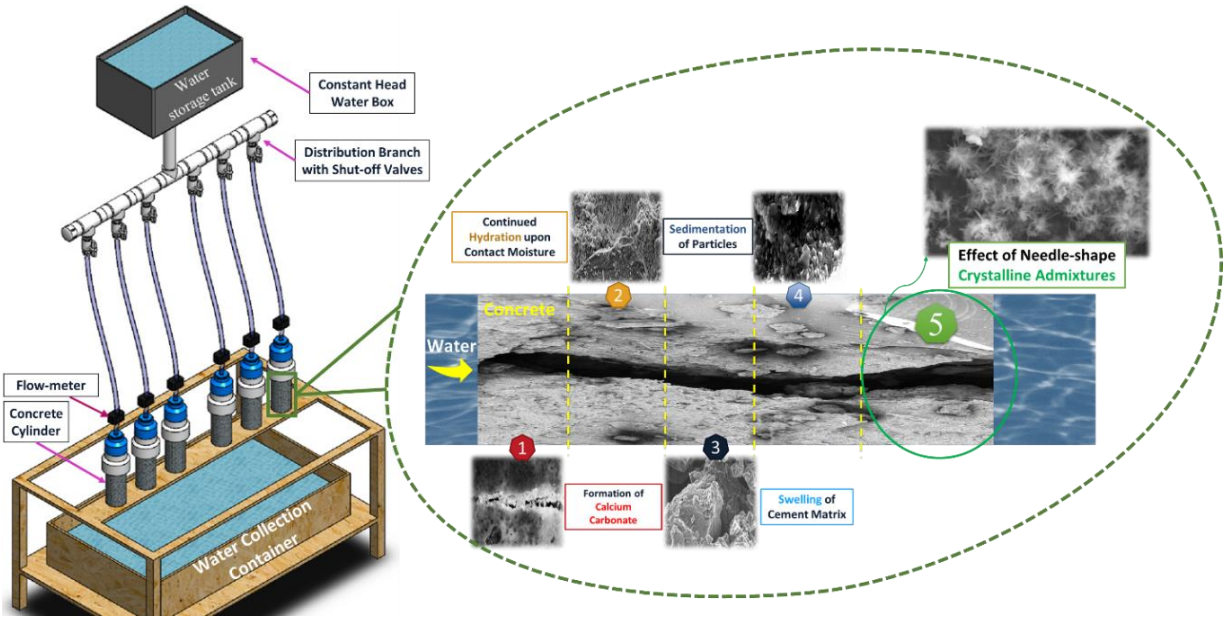

Fig. 1. Self-healing mechanisms [2] and testing setup.

$$3CaO - SiO_2 + M_xR_x + H_2O \rightarrow Ca_xSi_xO_xR - (H_2O)_x + M_xCaR_x - (H_2O)_x$$

(Calcium silicate + crystalline promoter + water→ modified calcium silicate hydrate + pore-blocking precipitate) Equation 1

There are a few recent studies that address the influence of CA as a promoter of SH. Jaroenratanapirom and Sahamitmongkol [53,54] studied the visual closing of cracks in mortar samples which were treated with crystalline and expansive admixtures and immersed in water for the healing period. Their results indicated that CA performed better than control mortars in healing of small (under 50 µm) and early age cracks (at 3 and 28 days) although showed ineffective behavior for larger cracks (300 µm). In a similar study, Sisomphon *et al*. [25] reported that only cracks up to 150 µm were completely sealed when pre-cracked cement-based materials treated with calcium sulfo-aluminate (CSA)-based expansive additive and CA were immersed in water for 28 days. Later, Sisomphon *et al*. [55] examined the recovery of mechanical properties of CA treated strain-hardening cementitious composites subjected to wet/dry cycles, humidity chamber, water immersion, and air exposure. Although, their results showed slight benefit of using CA as compared to control mixtures, the reaction was observed for both CA- and un-treated samples when exposed to wet/dry regime. Ferrara *et al*. [56] investigated the self-sealing capability and recovery of stiffness and load-bearing capacity by means of 3-point bending test, in normal strength concrete containing CA at a dosage of 1% by the cement weight. For water immersion condition, they reported that the presence of CA sped up the crack healing process and recovered the bending stiffness as well as load-bearing capacity of concrete. However, for specimens in accelerated exposure condition, no definite conclusion was stated due to high dispersion of obtained results. It was also found that a crack closure above 70-80% is necessary to start recovery of stiffness and load bearing capacity [56]. Influence of CA on the

concrete SH, measured by standard water permeability test after being subjected to four healing conditions, were tested by Roig-Flores *et al*. [57].. Water immersion (WI), water contact (WC), humidity chamber (HC), and air exposure (AE) were different environmental conditions utilized with the objective of simulating practical circumstances. They stated that neither control specimens nor those with CA healed when exposed to moist conditions. In their findings, four exposures in the order of decreasing permeability healing ratio were: WI (around 0.9) > WC (around 0.8) > HC (around 0.5) > AE (around -0.15) [57]. Afterwards, Roig-Flores *et al*. [58] studied the SH capability of early-age concretes containing 4% CA using water permeability test based on the standard procedure in EN 12390-8 [59]. They concluded that under water at 15 ºC and especially at 30 ºC, healing ratio was higher for CA treated specimens as compared to those for control. However, the highly-scattered results were seen for both treated and un-treated concrete under the wet/dry cycles exposure. In a recent study by Ferrara *et al.* [1], the effects of CA on the SH capacity of the cementitious composites with reference both to a normal strength concrete (NSC) and High Performance Fiber Reinforced Cementitious Composite (HPFRCC) were examined. In the treated mixture, a CA dosage of 3% was added and details of their experimental program were similar to those reported in [56]. In the case of both NSC and HPFRCC, CA enhanced and made the autogenous healing capacity of cementitious composites more reliable. In NSC, CA could promote up to 60% of crack sealing even under exposure to open air. In the case of HPFRCCs, which would already feature autogenous healing capacity because of their specific mix compositions, the synergy between dispersed fiber reinforcement and the action of the CA has resulted in a likely 'chemical pre-stressing' of the same reinforcement, from which the recovery of mechanical performance of the material has greatly benefited, up to levels even higher than the performance of virgin un-cracked material.

Although, efficacy of CA as a SH agent has been already documented and fairly well-understood, some discrepancies have been noted after reviewing the healing capability of concrete containing CA which motivates the specific analysis on this topic to enlarge the database available in current literature. In addition, an appropriate lab test method is required to help generate supporting data. For instance, in the above-mentioned studies where they used standard water permeability test to measure water penetration depth in pre-cracked concrete, the main requirement was to continuously subject the specimen to hydrostatic pressure which might not happen in practice and interfere with the results. However, an experimental methodology, schematically shown in Fig. 1 and developed in authors' previous study [60], can analyze real-life conditions of the self-healing process and directly quantify this mechanism. The innovative test technique involves three stages: (1) inducing repeatable cracks, (2) subjecting the cracked specimens to controlled hydrostatic pressure to measure flow, (3) quantifying the self-healing property of cement-based materials. Moreover, influence of CA on water permeability and durability properties such as chloride penetration resistance and electrical resistivity in virgin concrete mixtures especially when combined with Portland Limestone Cement (PLC) has yet

to be confirmed. Through crystalline deposition and densification of concrete matrix, it is expected that porosity reduces, resulting in lower permeability and enhanced ion diffusion resistance (e.g. chloride). However, to the authors' knowledge, no studies have discussed the chloride permeability and electrical resistivity of concrete with CA and therefore investigated herein for the first time. Limited experimental studies have been performed to find relationships between aforementioned test results of concrete which will be explored in this study as well.

The objective of the present study was to experimentally investigate the effectiveness of CA in enhancing SH mechanisms and improving the water and chloride penetrability characteristics of concrete. Penetrability properties were measured using rapid chloride permeability (RCP) test following procedures documented in ASTM C1202 [61], surface/bulk electrical resistivity test in accordance with AASHTO TP95 [62], bulk diffusion test according to ASTM C1556 [63], and DIN 1048 [64] test that determines the water permeability under hydrostatic pressure. Correlation and systematic comparison among these test methods were also established for concretes with CA. The well-standardized methodology was employed from authors' previous work [60] to evaluate the SH properties of cracked specimens based on measure of the flow rate through crack.

2. Experimental Program

This study investigated the effect of CA on durability and self-healing properties of concrete. This section comprises of a description of the materials, mixture proportions, casting, curing conditions and preparation of specimens including the testing procedures performed to determine the mechanical and certain durability properties of CA treated concrete.

2.1 Materials and mixture proportions

Two different cement classes, Ordinary Portland Cement (OPC) - Type I in accordance with ASTM C150 (referred as Type GU in CSA A23.1-14 [65]) and Portland Limestone Cement (PLC) (also referred as Type GUL in CSA A23.1-14 [65]), were investigated in this study, featuring the same water/cement (*w/c*) ratio and cement contents. The compositions of concrete mixtures utilizing two different cement types were further modified by adding CA, in powder form, by 2% of the weight of cement, and behavior was compared with control specimens without CA. A commercially available hydrophilic permeability reducing admixture (PRA) was used as the waterproofing cementitious material (or CA). The dosage utilized was as per the recommendation of the manufacturer and was also in accordance with what is used in field applications. Due to the proprietary nature of this product, its chemical composition is not available, however, it is known that this is a cement-based hydrophilic admixture that meets the specifications of ACI 212 [52] as described earlier. The *w/c* ratio used was 0.532 in all types of concrete mixtures and the mix design, which represents a typical

mix used in the field with target strength of about 35 MPa, is given in Table 1. The reference mixes are OPC and PLC and the ones containing CA are labeled as OPC-CA and PLC-CA respectively.

Table 1. Mixture proportions of concrete.

Mix ID	Mixture proportions (kg/m^3)					*w/c* ratio
	Cement	Aggregates		Water	CA (2%)	
		Coarse (5-14 mm)	Fine			
OPC	358	990	862	190	-	0.532
OPC-CA					7.16	
PLC					-	
PLC-CA					7.16	

2.2 Specimen preparation

For each mixture, in total, twenty cylinders of both Φ100×200 mm and Φ100×150 mm, and also three conical frustum of Φ150 (top)×175 mm for water permeability test were prepared in accordance with the recommendations of ASTM C192 [66]. In accordance with ASTM C143 [67], slump flow tests were performed within 15 minutes after the preparation of mixtures to avoid any loss of workability with time. For all mixtures, air content was also determined by following the procedures of ASTM C231 [68]. The density of a fresh concrete batch was also measured in accordance with ASTM C138 [69]; it is theoretically defined as the mass to volume ratio [69]. Temperature of fresh concrete mixture was measured in accordance with ASTM C1064 [70]. After 24±2 h, the specimens were removed from the molds, all Φ100×200 mm cylinders were continuously cured in a water bath before testing while other samples were air-cured. Table 2 summarizes the specimens' type and quantity as well as curing conditions used in different test methods.

Table 2. Type, number, and curing conditions of specimens used in different test methods.

Test method	Number of specimen	Type of specimen	Curing condition	Standard
Compressive strength	3	Cylinder (Φ100×200 mm)	28 days (water-cured)	ASTM C39
Water permeability	3	Conical frustum (Φ150 [top]×175 mm)	28 days (air-cured)	DIN 1048
Electrical resistivity	3	Cylinder (Φ100×200 mm)	210 days (water-cured)	AASHTO TP95
Rapid chloride permeability	4	Cylinder (Φ100×50 mm)	28 & 56 days (water-cured)	ASTM C1202

Apparent diffusion coefficient	3	Cylinder (Φ100×75 mm)	28 & 56 days (water-cured)	ASTM C1556
Self-healing	10	Cylinder (Φ100×150 mm)	28 days (air-cured)	-

2.3 Methodology and parameters investigated

2.3.1 Compressive strength

At 28 days from casting, three cylindrical specimens (Φ100×200 mm) from each mixture were tested in saturated surface dry (SSD) condition, following the procedure reported in ASTM C39 [71] in order to determine each mixture's compressive strength.

2.3.2 Electrical resistivity (surface and bulk resistivity)

Non-destructive electrical resistivity measurement was performed on three Φ100×200 mm cylinders at the ages of 7, 14, 28, 56, 90, 160, 210 days. The surface electrical resistivity (SR) measurement, following both AASHTO TP95 [62] and ASTM working document (WK37880) methodologies, was performed by two commercially available non-destructive four-probe (equally spaced at 38 mm) Wenner SR meter. . The equipment, shown in Fig. 2-(a) works on low fixed frequency alternating current (AC) which is flowing between the outer electrodes and measures the potential difference between two inner electrodes. This study also investigated the influence of different frequencies (13, 40, 100 Hz) and two commercial SR meters. All cylinders were removed one by one from the water curing tank before testing on the specified test days and were tested at SSD condition at 23±3 °C. A total of eight measurements with the four set of probes centered every 90° along the longitudinal direction of cylinder were recorded.

Another non-destructive resistivity-meter was used to measure the Bulk Resistivity (BR) of the same Φ100×200 mm concrete cylinders (Fig. 2-(b)). Since resistance measurement with a DC signal is not recommended due to electrodes' polarization effect [62], an alternating current (AC) was used to apply the current at a fixed frequency of 1 kHz through the specimen. Previous work by Yildrim *et al.* [72] and Al-Dahawi *et al.* [73] indicates that the polarization effects in the material can be neglected when the frequency is at least 1 kHz. The electrodes consist of circular stainless-steel plates, on which a contact sponge wetted with a dilute solution of soap, was inserted in between two electrodes to ensure that the entire surface is in electrolytic contact with the electrode. Fig. 2 also shows a schematic diagram of fundamental physics involved for the measurement of the SR and BR. For each test, three specimens were tested, and average of these readings was further analyzed.

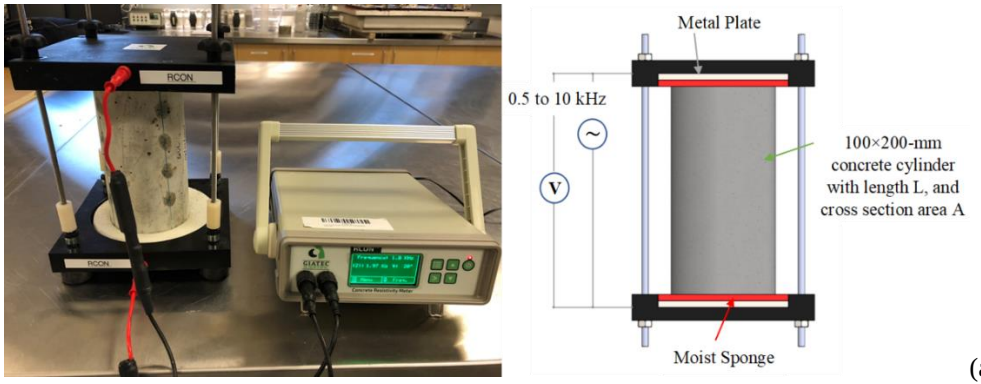

Fig. 2. Testing arrangement and schematic diagram of (a) BR meter (b) SR testing instrument.

2.3.3 Rapid chloride permeability (RCP) test

Following procedure reported in ASTM C1202 [61], the RCP test was performed on four concrete slices with 50-mm thickness, cut from four Φ100×200 mm cylinders. To ensure one-directional penetration of Cl^- ions, the side surfaces around the circumference of concrete slices were epoxy-coated. Afterwards, the disks were vacuum saturated (for 3 hours), deaerated, and then submerged in water for 18±2 h before testing (Fig. 3).

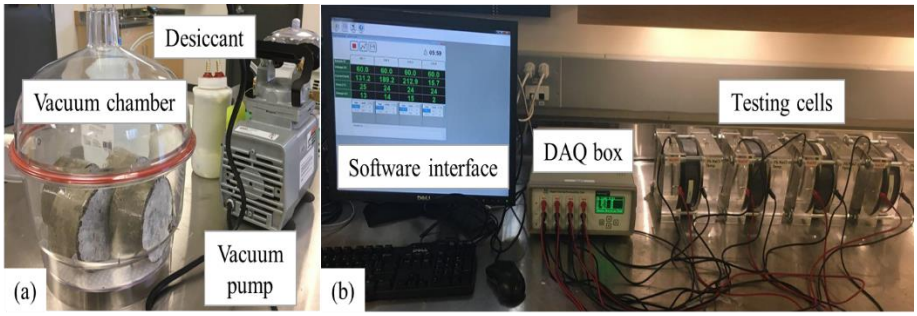

Fig. 3. (a) Water saturation setup (b) RCP test apparatus.

Specimens were then mounted into test cells of the device containing two reservoirs, where one reservoir was filled with 0.3 normal NaOH solution (anode), and the other with 3% wt. NaCl solution (cathode). 60 V potential difference was applied during the test to allow the transfer of chloride ions through concrete from cathode (NaCl solution) to anode (NaOH solution). The test was conducted for a six-hour period, during which the current and temperature were measured every minute. The total

charge passing was measured by integrating the area under current vs. time curve, presented in Coulombs and the average value of four samples was reported.

2.3.4 Water permeability coefficient

The water permeability of mixtures was determined using DIN-1048-Part 5 standard [64]. Prior to testing, specimens' top surface was wire brushed, following the DIN 1048 standard, and then three specimens from each mixture were subjected to 0.5 MPa (5 bar) of hydrostatic pressure for three days (72 h). Each specimen was mounted into a cell consisting of a rubber gasket with a 100-mm diameter to avoid leakage while applying water pressure. After the testing was completed, the specimens were split into two halves (perpendicular to the injected face) using a compression machine and the depth of water penetration was marked for each half and measured immediately.

Assuming that the flow of water through the concrete pores is stationary and laminar [74], coefficient of water permeability (k_w) can be determined using measured water depth according to modified Darcy's Law [74] as follows:

$$\frac{dx}{dt} = k_w \frac{h}{x} \qquad \text{Equation 2}$$

where x is the penetration depth (m), t represents the experiment time (s), k_w indicates the permeability coefficient (m/s), and h is the water head (m). Permeability coefficient can be simply derived by integrating Equation 2to obtain Equation 3:

$$k_w = \frac{x_t^2}{2ht} \qquad \text{Equation 3}$$

where x_t is the penetration depth at time *t.* Since the water flow is unsteady and associated with sorptivity, it is more reasonable to consider average depth of water penetration instead of maximum one to calculate k_w [74]. Using AutoCAD software, the x_{avg} for divided specimens was determined by measuring the wetted area (A_w) and maximum width (w_{max}) of this region as illustrated in Fig. 4. Then, x_{avg} was calculated as the average of the A_w divided by w_{max} for each half.

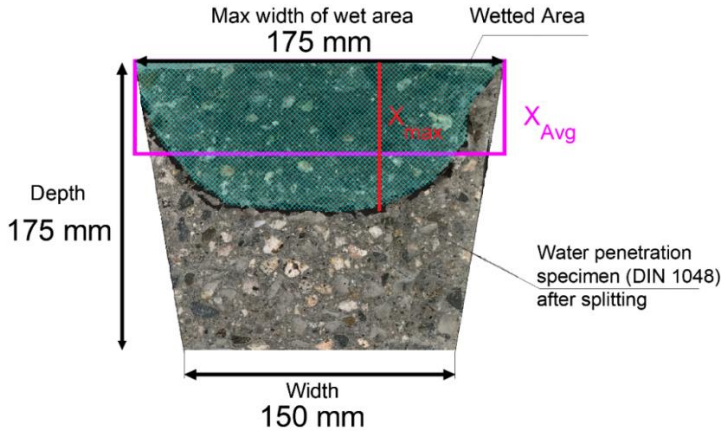

Fig. 4. Method for calculating the average depth (x_{avg}) in the wetted region.

2.3.5 Apparent chloride diffusion coefficient

To determine the values of surface chloride concentration and apparent chloride diffusion coefficient for each mixture, Φ100×200 mm cylinders were sliced into 75 and 20 mm-thick disks cured inside the water curing tank for 28 and 56 days. After the curing period, specimens were air-dried, sealed from all sides except the finished surface, immersed in a saturated calcium hydroxide (3 gr/L) water tank until the mass did not change by more than 0.1 % in 24 h; later ponded in 165 gr/L aqueous NaCl solution according to ASTM C1556 [63] for 6 months at 23±3 °C. The specimens' weight before and after ponding were measured. After ponding, samples were removed from the solution and stored for 24 h in the laboratory at 23±3 °C and 50±4% RH. Using a rotatory hammer drill, 10 grams of powder sample were obtained from each layer by grinding off the material parallel to the exposed surface. To determine acid-soluble chloride-ion content of powder mass, C_x (mass %), rapid chloride test (RCT) kit was used.

2.3.6 Self-healing test

As mentioned earlier, ten cylinders of Φ100×150 mm for each mixture were prepared. These were later cracked using an innovative technique reported by authors in [60] in order to examine self-healing capability of cracked cylinders. One of the major benefits of this method is to use simple and readily available specimens that are commonly prepared for determining resistivity and compressive strength of concrete. All cylinders were kept in the laboratory and cured in ambient temperature prior to cracking. After curing, each sample was placed in a standard crack-inducing jig (SCIJ) to induce a crack width ranging from 0.1 to 0.4 mm using a universal testing machine. The SCIJ consists of two V shaped cutting edges that act as stress concentrators and are connected to the top and bottom plate of the jig. Spring loaded side aligning strips exert a lateral compressive force that prevents complete splitting of the sample, which is essential to simulate real world situations. The specimens are placed along their length and indirect tension is induced through the cutting edges. The tortuosity of the cracks and the interlocking of the aggregates prevent the specimens from splitting after cracks are produced. Surface crack width for each cylinder (top and bottom ends) was measured by an optical crack-detection microscope at 14 equidistant points along the crack: seven along the top face, and seven along the bottom face. The measurements were then averaged and recorded as the cylinder average. The cracked specimens were later inserted into special rubber sleeves, sealed using silicon sealant; then one end of cylinder sample was exposed to a constant water head (~ 1.7 m). The flow of water through specimens was collected in water containers and measured over a period of time (Fig. 1).

3. Results and discussion

This section is aimed to show the influence of CA addition into concrete with two different cement types on the strength, electrical resistivity, water permeability, electrical charge passed based on RCP

test, chloride diffusivity. In addition, several correlations of these durability parameters were established. Self-healing efficiency of all mixtures was also demonstrated using an innovative technique developed by the authors.

3.1 Fresh concrete properties and compressive strength results

The experimental results of the concretes with and without CA including fresh properties (slump, air content, and plastic density), compressive strength, and electrical resistivity is summarized in Table 3. Compressive strength and electrical resistivity results, determined at 28 days, are the average from three cylinders (Φ100×200 mm). As indicated by the results in Table 3, the addition of CA increased the compressive strength by 11% for OPC mixture and by 8% for PLC mixture, while not much significant increase has been observed for electrical resistivity data (both SR and BR).

Table 3. Fresh and hardened concrete properties.

Mix ID	**Fresh properties**				**28- day compressive strength (MPa)**	**28-day electrical resistivity (kΩ.cm)**	
	Slump (mm)	Air content (%)	Plastic density (kg/m^3)	Temperature (°C)		Surface	Bulk
OPC	130	2.0	2400	21.0	41.54	6.75	4.01
OPC-CA	110	2.2	2394	21.0	46.35	6.47	4.06
PLC	130	1.9	2394	20.5	42.07	6.12	3.91
PLC-CA	85	2.2	2396	21.0	45.62	6.61	4.03

One possible reason for the increase in compressive strength with CA can be associated with a filler effect that can contribute to close the voids but can also work as a cement hydration activator by improving the paste cement microstructure. In addition, presence of CA in the mix indicated a reduction in slump values whereas a slight increase in the air content was observed. Due to hydrophilic nature of CA used, it has tendency to absorb more water during mixing process which results in lower workability and inducing more air bubbles in the mix.

3.2 Electrical resistivity results

The surface and bulk electrical resistivity of concrete with and without CA at 7, 14, 28, 56, 90, 160, 210 days are illustrated in Fig. 5. Generally, as concrete aged, resistivity increased due to further cement hydration and due to the progressive hardening of concrete. Other studies also reported similar trend [73-80] although none of them studied the effect of CA addition or PLC in the mixture. Dependency of resistivity of concrete on its microstructure properties as well as conductivity of its pore solution, proves increase in resistivity over time since concrete's interconnected pore network

reduces and OH^- ions in the pore solution is consumed, attributing to decrease in its conductivity. Table 4 summarizes the chloride permeability classifications for electrical resistivity and RCP test methods. According to the classifications given in this table, electrical resistivity results correspond to high chloride permeability. It can be observed that addition of CA helped concrete to slightly enhance its SR over time; showed greater resistivity values (especially for PLC mixtures) than that of control mixtures. Comparing the reference cylinders containing only Portland cement, the SR and BR of mixtures with limestone was lower (less than 10%) than that of ordinary ones for all ages tested. Concrete resistivity typically increases with time and can be expressed by:

$$\rho(t) = \rho_0 \left(\frac{t_0}{t}\right)^{-m} \quad \text{Equation 4}$$

where $\rho(t)$ and ρ_0 is the concrete resistivity at time (t) and reference time (t_0), respectively; m is the ageing factor ($0 \leq m \leq 1$) which depends on concrete composition and environmental conditions. The ageing factor, (m), determined using Equation 4 with a reference age of 7 days (t_0) and the concrete resistivity measured at that age ρ_0, are dependent on microstructure changes over time. As illustrated in Fig. 5, the fitting curves are plotted by dash-lines and the growth of SR and BR have a common rate of development trend while SR measurement represented better correlation than that of BR method according to its coefficient of determination (R^2), suggesting less dependency of this method on the testing and concrete parameters. While presence of CA could lead to higher SR values, it showed a slight decrease in BR data as compared to reference samples. This cannot be necessarily rooted from incorporation of CA in the mix as BR measurement technique is considerably dependent on sponge contact, surface-to-electrode contact, degree of saturation, etc. Considering only SR measurements, a strong correlation between SR and curing age has been established ($R^2 > 0.93$), indicating reliability of proposed equations to predict SR evolution over time. A fair correlation (R^2 = 0.53 and 0.74) was also observed for PLC mixtures measured using bulk resistivity method while the correlation for OPC mixtures was poor. For OPC mix, BR data was randomly distributed over time that m value could not be obtained after several iterations in regression analysis. All fitted curves in the BR graph could not cover all data points due to larger scattering in the results. This could not be fulfilled by adjusting the data into Equation 4. Generally, concretes containing crystalline admixtures did not show any considerable differences in enhancing electrical resistivity when compared to control mixtures. It should be noted that measuring concrete electrical resistivity is an indirect testing technique to obtain information about its permeability which might not be an appropriate way to understand CA behavior under permeation or diffusion. Hence, this study also investigates other durability evaluation techniques to draw some comprehensive conclusions about the aspects of using CA or to determine which technique can truly represent real behavior of CA in a concrete system.

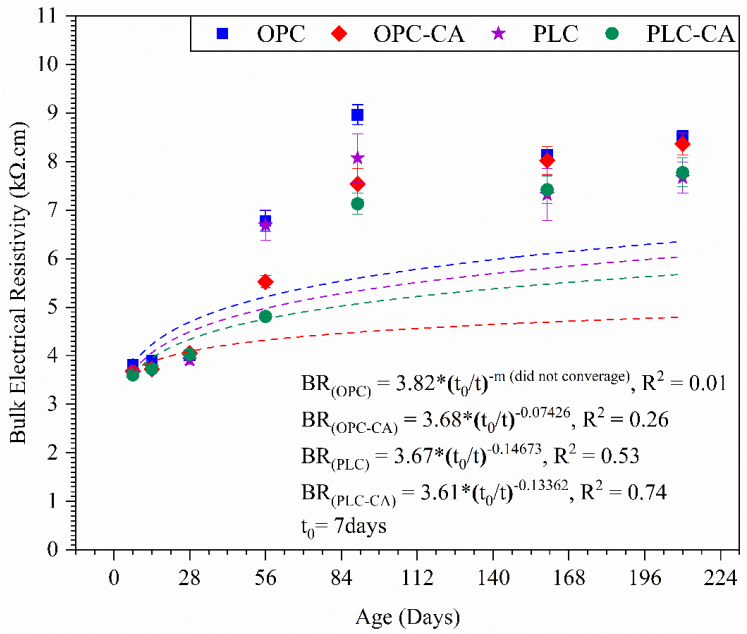

(a) BR data

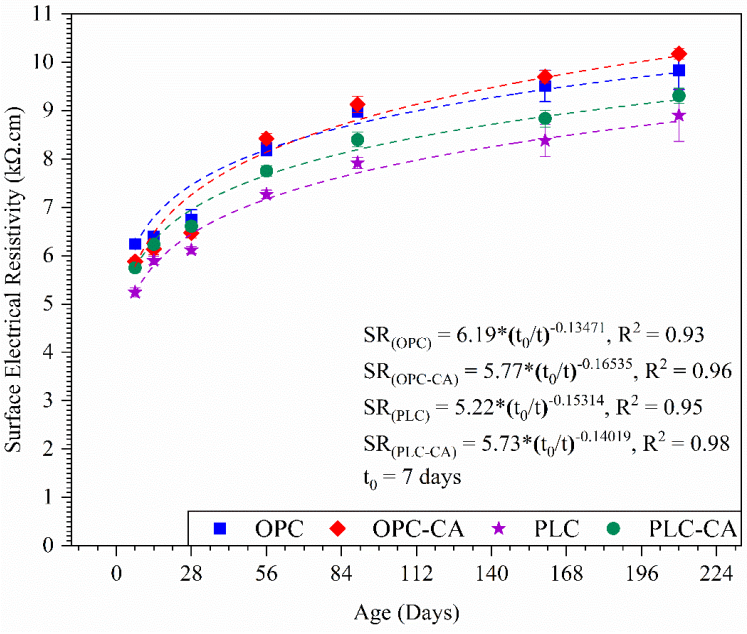

(b) SR data

Fig. 5. (a) Bulk and (b) surface electrical resistivity variations over time.

Table 4. Chloride permeability classifications.

Chloride permeability	**RCP [58] test (Coulomb)**	**Electrical resistivity (kΩ.cm)**		**Diffusion coefficient (10^{-12} m^2/s)**
		Surface [62]	Bulk [77]	
High	> 4000	> 12	> 5	> 15
Moderate	2000 – 4000	12 – 21	5 – 10	10 – 15
Low	1000 – 2000	21 – 37	10 – 21	5 – 10
Very Low	100 – 1000	37 – 254	21 – 207	2 – 5

Negligible	< 100	< 254	< 207	< 2

Amongst various parameters, signal frequencies are known to have an effect on resistivity of concrete. This effect of signal frequencies on SR data was investigated using three different signal frequencies (13, 40, and 100 Hz) in the 4-point Wenner method. No significant difference in SR results among different signal frequencies was observed and as frequency increased, less than 5% reduction in the SR values was detected.

3.3 Rapid Chloride Permeability (RCP) test results

The chloride permeability was measured by RCP test as acid-soluble chloride (total chloride), in accordance with ASTM C1202 [61]. Fig. 6 presents the results of RCP test for individual specimens in each mixture as well as their average values taken from four samples. The average cumulative charge after 6 h was 5538 Coulombs for OPC at 28 days, and was approximately 25%, 35%, and 30% higher for OPC-CA, PLC, and PLC-CA, respectively. This was 2315 Coulombs for OPC at 56 days, roughly 5% higher than OPC-CA, and was ~11% and 19% lower for PLC and PLC-CA mixtures, respectively. Based on these results, the charge passed reduction in all mixtures over time (28 to 56 days) can be attributed to the reduction of the pore volume as well as pore solution chemistry. Similar findings have been reported in other studies [74], [81-87] for OPC mixtures although none of these studies examined the crystalline admixtures' effect. It should be noted that one of criticism of the RCP test is that an increase in temperature is resulted from the high voltage applied across the sample, especially for low quality concretes, which is known to lead to an increase in charge passed, resulting in poor quality concrete looking worse than it actually is [88]. Addition of CA into OPC mixture induced a significant decrease in the charge passed at 28 days but did not result in a major change at 56 days. One would actually expect the opposite trend since the CA addition over time is known to support formation of needle-shaped crystals which act as a physical membrane to prevent passage of water inside the concrete matrix. Since the test error inherently associated with the RCP test is larger than any effect of CA addition, no definitive conclusions can be drawn. In contrast the inclusion of CA into PLC mixture indicated slightly higher value than control one (PLC mix), representing the uncertainties inherent in the test method. The enhancement of the resistance to chloride penetration in OPC-CA mix can be related to the capillarity and pore volume reduction as well as microstructural characteristics of this mix, formed by the deposition of pore blocking crystals inside the matrix. Comparing only OPC and PLC mixtures, it can be observed that cement composition can affect the electrical conductivity of the pore solution and matrix, resulting in lower value for PLC mix at 28 days (Fig. 6). At the age of 28 and 56 days, RCP results indicate high and moderate chloride permeability for all mixtures based on the classification in ASTM C1202 [61], presented in Table 4. Based on the obtained RCP data, only definite conclusion is that the total charge dropped in all mixtures from high to moderate range from 28 to 56 days.

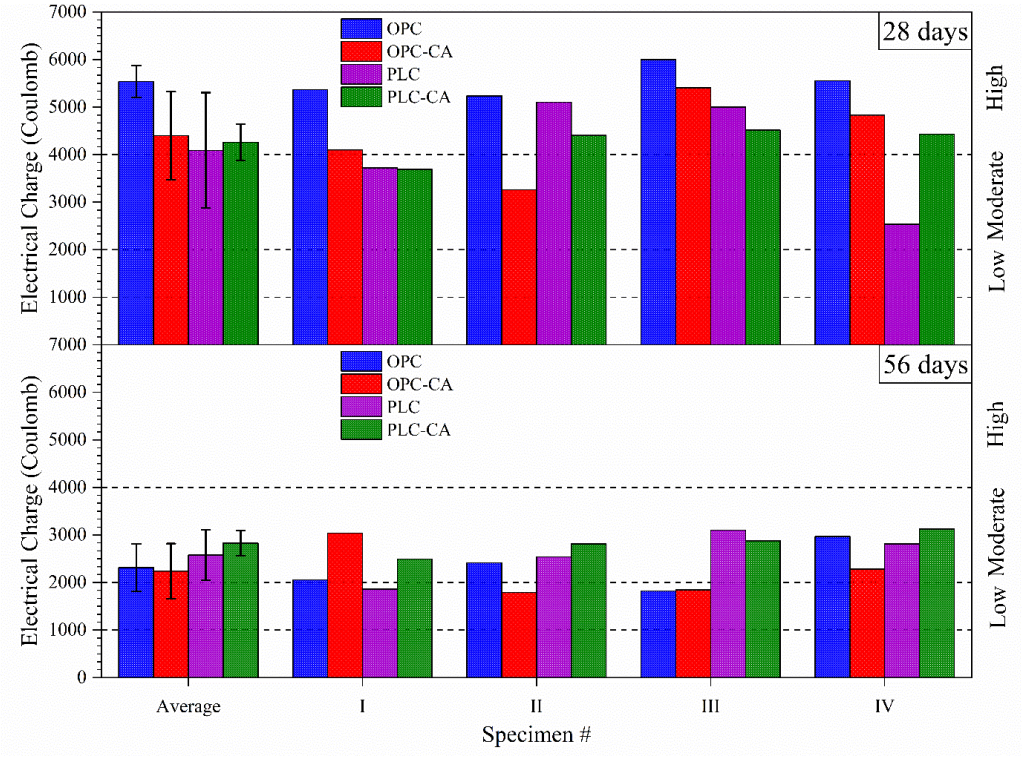

Fig. 6. RCP test results (electrical charge passed [Q] in Coulomb) at 28 and 56 days.

3.4 Water permeability test results

The ease of water penetration into the concrete usually determines its deterioration rate while affects its durability [89]. Generally, the lower the concrete permeability, the higher its durability. To evaluate the concrete permeation, water penetration test in accordance with DIN 1048-Part 5 [64] has been utilized in this study. After performing the water penetration test for a period of 72 h and splitting the specimens into two halves, average and maximum depth of water penetration (x_{avg} and x_{max}) were measured as illustrated in Fig. 7. It can be simply observed that incorporation of CA into concrete significantly reduced water penetration depth. For all concrete mixtures, Fig. 8 exhibits the average and maximum depth of water penetration as well as their permeability coefficients ($k_{w(avg)}$ and $k_{w(max)}$, calculated from Equation 3) based on DIN 1048 test results. As can be seen in Fig. 8, the penetration depth reduced considerably (40-50%) for concretes treated with CA, indicating the effectiveness of these admixtures for waterproofing purposes. According to Hedegaard and Hansen's study [90], concrete can be considered as watertight for all practical purposes when maximum penetration depth is less than 50 mm.

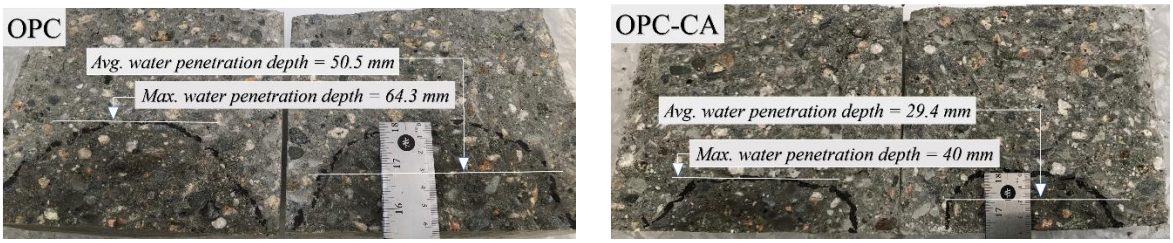

Fig. 7. Water penetration depths of concretes with and without CA.

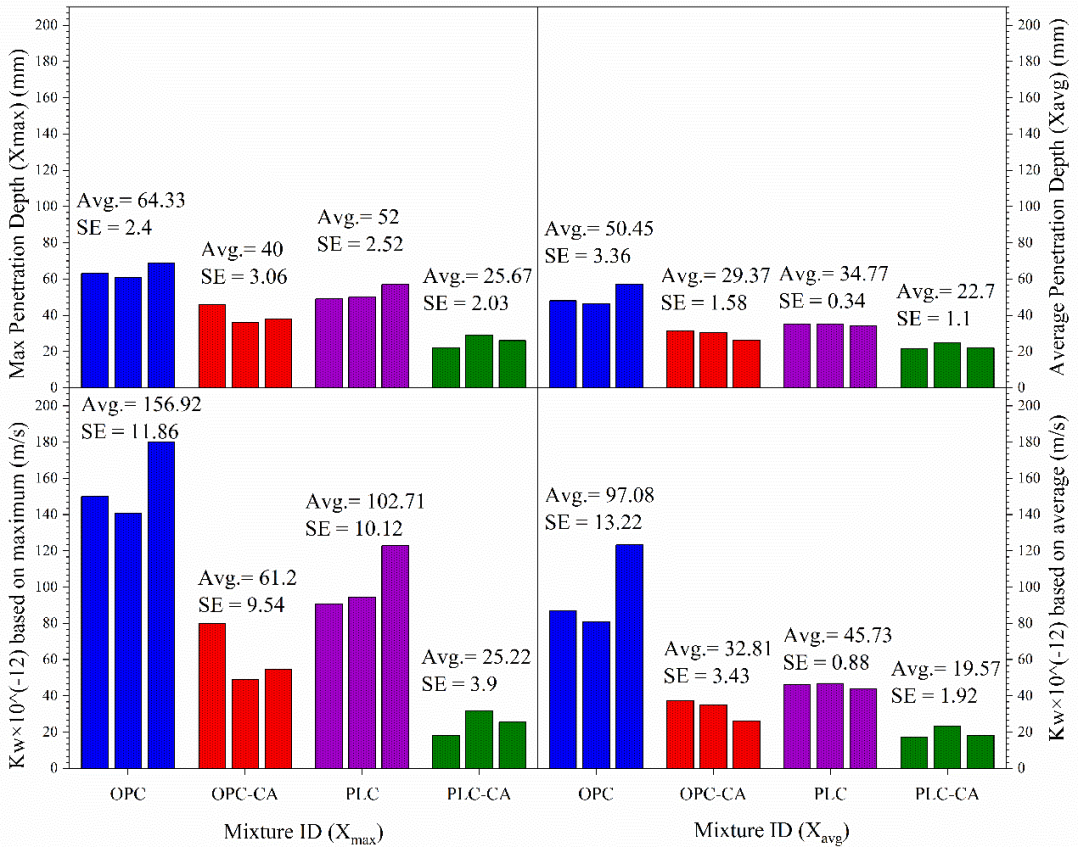

Fig. 8. Mixtures' water penetration depth and coefficient of permeability based on DIN 1048 test results.

Only CA treated mixtures satisfy this statement by having the average values of 40 mm for OPC-CA and 25.7 mm for PLC-CA. Comparing the water penetration depth based on maximum or average values, it was observed that standard errors of results were lower for average penetration depth, suggesting reliability of using average depth instead of maximum one. OPC mixture (control one) showed the highest penetration depth, as result the highest permeability coefficient (k_w), followed by PLC, OPC-CA, and PLC-CA. According to obtained results, the mixture of PLC-CA indicates the highest resistance to water penetration when compared to other mixtures. When only reference mixtures are considered, PLC showed noticeably higher water tightness than that of OPC (~25% improvement). It should be noted that no similar study has been found to investigate the role of PLC on concrete waterproofing.

3.5 Chloride diffusion coefficient

For all mixtures exposed to bulk diffusion in NaCl solution for 180 days, the values of chloride content (Cl^-% of concrete weight) vs. layer depth (mm), measured at 2.5, 8, 14.5, and 21.5 mm depth from concrete surface, are plotted in Fig. 9-(a) where specimens, shown on the left side, were cured for 28 days in water and on the right side for 56 days prior to exposing to NaCl solution. The best-fit

curves are also shown by dash-lines in the same plot and their slopes decrease as concrete ages. It was observed that specimen curing time can affect the penetration of chloride ions into different depth, mostly due to gradual improvement in the extent of the concrete hydration, density and inner pore structures with time. Besides that, different diffusing ions clogged the pores inside concrete, not allowing further diffusion of chloride ions and resulting in concrete's higher capacity to withstand chloride diffusion; thus, leading to a low chloride concentration. Hence, the more concrete cures with moisture in a marine environment, it will be less prone to chloride attack. Overall, for both curing ages, the chloride content values were lower for specimens treated with CA than that of control mixtures, suggesting formation of crystalline structures inside pores that act as physical barrier and can increase chloride binding capacity of matrix; also, can decrease penetration depth of water carrying chloride ions into concrete. As shown earlier, water penetration depth was lower in concrete containing CA. Comparing two cement types showed ~15-20 % higher chloride content at all depths for PLC mixtures. The service life of concrete in a chloride environment can be explained by Fick's second law. Using chloride ions' content profile and the method of least square, the values of surface concentration and apparent diffusion coefficient were determined by fitting the following equation (Fick's second law) [63]:

$$C(x,t) = C_s - (C_s - C_i) \cdot \mathrm{erf}\left(\frac{x}{\sqrt{4 \cdot D_a \cdot t}}\right) \qquad \text{Equation 5}$$

where $C(x,t)$ is chloride concentration measured at depth x and exposure time (t = 6 months) in mass % of concrete; C_i is initial chloride-ion concentration of the cementitious mix before salt solution submersion; C_s is projected chloride concentration at the interface between the exposure liquid and cylinder finished surface and D_a is apparent chloride diffusion coefficient in m^2/s which both parameters are determined by nonlinear regression analysis. The resulting chloride surface contents and diffusion coefficients are illustrated in Fig. 9-(b) for all mixtures at 28 and 56 days. The calculated surface contents ranged from 0.8% to 2% with higher contents belonging to specimens cured for 28 days and not treated with CA. Those for OPC and PLC (1.6-1.8%) mixtures were higher than for OPC-CA and PLC-CA mixtures. It was observed that C_s of all mixtures decrease with an extension in the curing age. The chloride typically penetrates into concrete through capillary absorption and diffusion [91,92]. The C_s mainly depends on capillary absorption of chloride [93] and until saturation occurs in capillaries, concrete absorbs saltwater. The calculated apparent diffusion coefficients range from 4 to 14×10^{-12} m^2/s. These values correspond to moderate/low chloride permeability according to classifications given in Table 4. Without any exception, the results indicate that OPC/PLC-CA have the lowest diffusion coefficient at both 28 and 56 days while value difference in OPC control and treated mixtures are relatively small at 56 days. It is interesting that specimens containing crystalline admixtures exhibited lower diffusion coefficient, indicating lower rate of

chloride ingress into matrix. These results corroborate well with the trend observed using the permeability test. As more hydration occurred, the modified C-S-H gel and needle-shaped crystals were produced in the pores of the capillary, which in turn increased the amount of hydration products and reduced the porosity and pore diameter in CA treated system. Hence, the concrete enhances its binding capacity with chloride ions and also its diffusion coefficient increases. This result suggests noticeable differences in chloride binding capacities between CA-treated and control concretes. These preliminary data cannot be taken as conclusive evidence to support this theory, but definitely shows the need for further exploration. The following equations can be used to estimate chloride profile and diffusion coefficient of concretes incorporating CA or PLC after t = 6 months of salt solution exposure:

$C(x,t)_{OPC-28D} = 1.786 - 1.781 \cdot \mathrm{erf}\left(\frac{x}{2 \cdot \sqrt{13.4t}}\right)$	OPC (28-day curing)	Equation 6
$C(x,t)_{OPC-56D} = 0.918 - 0.913 \cdot \mathrm{erf}\left(\frac{x}{2 \cdot \sqrt{5.25t}}\right)$	OPC (56-day curing)	Equation 7
$C(x,t)_{OPC-CA-28D} = 1.292 - 1.287 \cdot \mathrm{erf}\left(\frac{x}{2 \cdot \sqrt{6.28t}}\right)$	OPC-CA (28-day curing)	Equation 8
$C(x,t)_{OPC-CA-56D} = 0.843 - 0.838 \cdot \mathrm{erf}\left(\frac{x}{2 \cdot \sqrt{4.83t}}\right)$	OPC-CA (56-day curing)	Equation 9
$C(x,t)_{PLC-28D} = 1.903 - 1.898 \cdot \mathrm{erf}\left(\frac{x}{2 \cdot \sqrt{11.2t}}\right)$	PLC (28-day curing)	Equation 10
$C(x,t)_{PLC-56D} = 1.796 - 1.791 \cdot \mathrm{erf}\left(\frac{x}{2 \cdot \sqrt{8.66t}}\right)$	PLC (56-day curing)	Equation 11
$C(x,t)_{PLC-CA-28D} = 1.216 - 1.211 \cdot \mathrm{erf}\left(\frac{x}{2 \cdot \sqrt{9.77t}}\right)$	PLC-CA (28-day curing)	Equation 12
$C(x,t)_{PLC-CA-56D} = 1.203 - 1.198 \cdot \mathrm{erf}\left(\frac{x}{2 \cdot \sqrt{6.51t}}\right)$	PLC-CA (56-day curing)	Equation 13

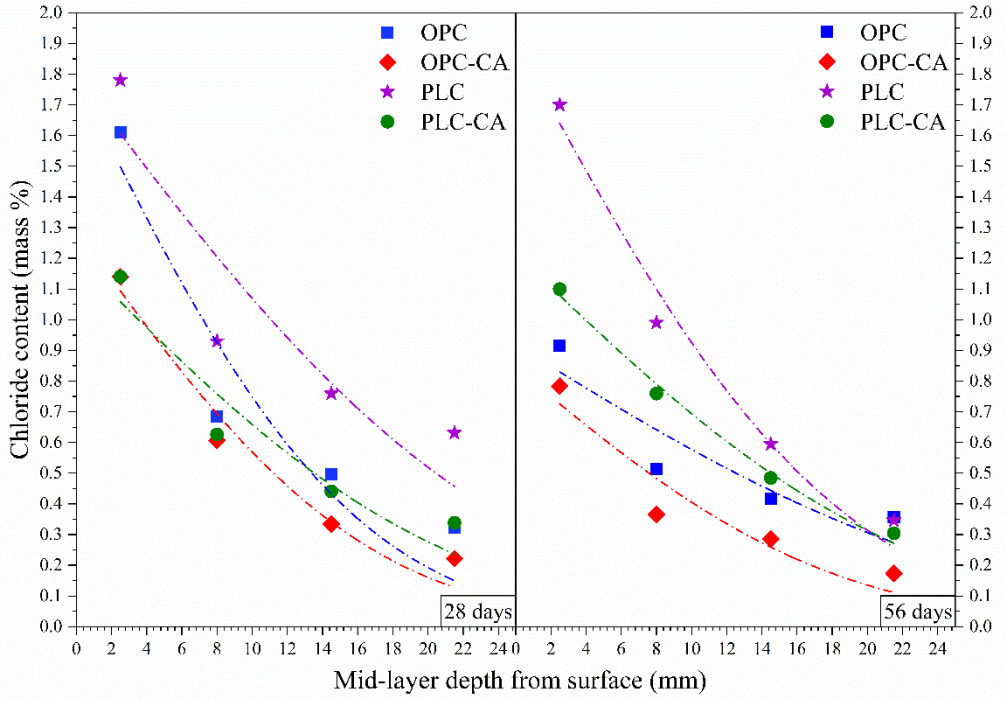

(a)

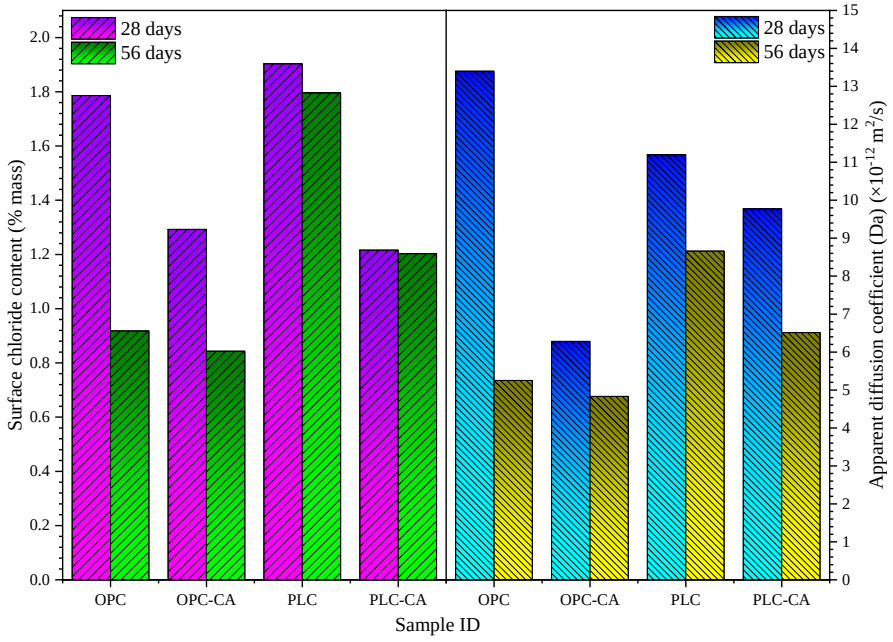

(b)

Fig. 9. (a) Chloride content profiles, (b) surface chloride concentration and diffusion coefficient for different concrete mixtures.

3.6 Inter-relationship between permeation properties and durability of concrete

In this section, any possible correlation between different durability indicator parameters such as ER and RCP is investigated. OPC and PLC concrete types are considered as the reference mix in this section and while OPC-CA and PLC-CA mixes are regarded as the CA mix. These two sample types are compared with each other through this section.

3.6.1 *Correlation between surface and bulk electrical resistivity*

Considering all curing ages, Fig. 10 shows the relationship between SR and BR data for all mixtures. Linear equation was the best regression fit to correlate the SR and BR data. As can be seen, two measurement techniques correlate fairly well (R^2 = 0.84) with each other for all cylinders. This finding agrees with the results reported in other studies [76,77]. Ignoring the limited application of BR testing technique for field evaluation, it is worth mentioning that the two test methods can be used interchangeably to measure concrete resistivity in the laboratory.

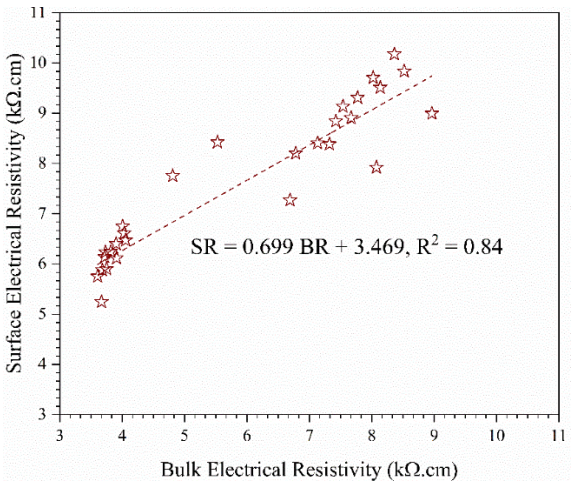

Fig. 10. Relationship between surface and bulk resistivity of both concretes with and without CA.

3.6.2 *Correlation between surface/bulk resistivity and RCP*

Fig. 11 shows the overall relationship between the charge passed and SR (or BR) measurements for CA-treated and control mixtures at 56 days. Each data point on the figure represents test results from a single specimen. There was also a good relationship between the SR measurements for both CA-treated and control concretes at 56 days. Similarly, results were also analyzed for all mixes at 28 days, but plots are not included to maintain brevity. Correlating 28 days SR/BR and RCP test results, the CA group showed strong linear relationship between these test methods while poor correlation was observed for control samples. The present research is among few studies investigating the correlation between RCP test and resistivity values [71,84,85,94]. Other studies suggest the use of power function to fit the data although it happened not to be a suitable fitting curve for this data set. This might be due to the high *w/c* ratio and small variations in RCP test and SR/BR results at certain age, not having wider range of data set. Generally, SR measurement indicated better correlation with RCP test than that of BR measurement.

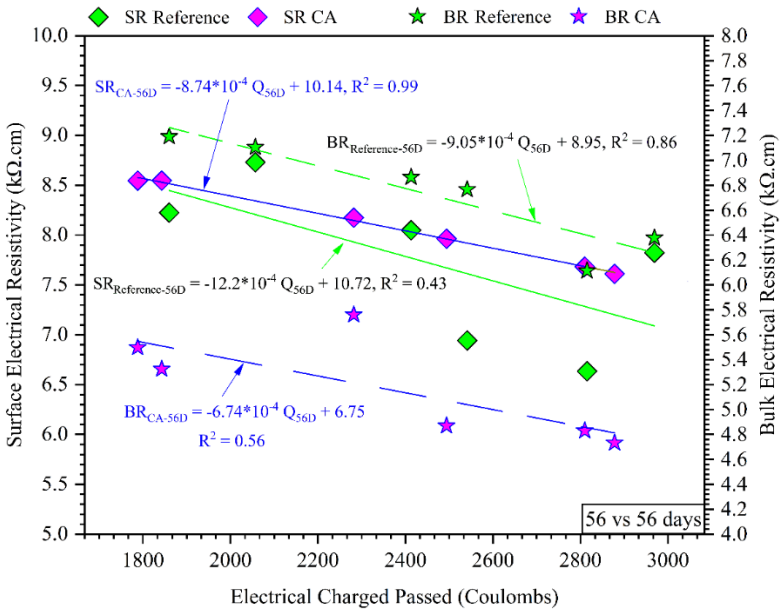

Fig. 11. Relationship between RCP test and surface (or bulk) electrical resistivity for CA and reference control mixtures 56 vs. 56 days.

3.6.3 Correlation between surface/bulk resistivity and water permeability

For all mixtures, the relationship between concrete resistivity obtained at 7, 28, and 56 days age and its water permeability coefficient measured based on maximum penetration depth was analyzed. The results indicated no linear relation between these parameters. No linear relationship was also found between resistivity and k_w measured based on average penetration depth. Fair correlation was observed only at 7 days and specifically for BR data. This is mostly due to air curing of water permeability test samples after casting. Previous studies showed the proposed relationship between these parameters [84,85]. Concretes containing CA showed no significant correlation between resistivity and water permeability when compared to control mixtures. As reported earlier, presence of CA in concrete led to considerable reduction in water permeability but no significant difference in resistivity values which is a possible cause not to find any meaningful correlation between these techniques. This also suggests that practitioners who frequently deal with these test methods should be cautious not to implement these techniques interchangeably for different cement-based mixtures. This is because the permeability test is a direct method to physically estimate the water penetration depth and permeability coefficient while resistivity method is an indirect technique to obtain information on permeability based on electrical resistivity of a porous medium.

3.6.4 Correlation between RCP and water permeability

The charge passed based on the RCPT results at 28 and 56 days were correlated with the k_w, calculated based on the x_{avg} and x_{max} measured using DIN 1048 test. Moderate linear relationship between Q and k_w was identified for both CA-treated and control concretes at 28 days; however, there was almost no correlation between these parameters at 56 days ($R^2 < 0.15$). A similar conclusion can be found in the literature [72,84,85]. Even though, CA-treated concretes showed better performance in

water penetration and RCP tests, they did not establish any significant relation between two parameters as compared with control samples. Further investigation is required to validate this relationship with wider range of testing specimens including different *w/c* ratio, curing age/regimes, and cementitious combinations.

3.6.5 Correlation between apparent diffusion coefficient and other durability parameters

To analyze the interdependence between concrete rapid chloride penetration, resistivity and chloride diffusion coefficient, the correlation between them was studied. Fig. 12-(a), (b), (c) show the relationship among chloride diffusion coefficient and other parameters measured through RCP, WP, and ER tests. Linear equation in the form of $y = ax \pm b$ was used for regression analysis in all cases as the best correlation. All parameters indicated poor correlation with D_a (R^2 <0.6).

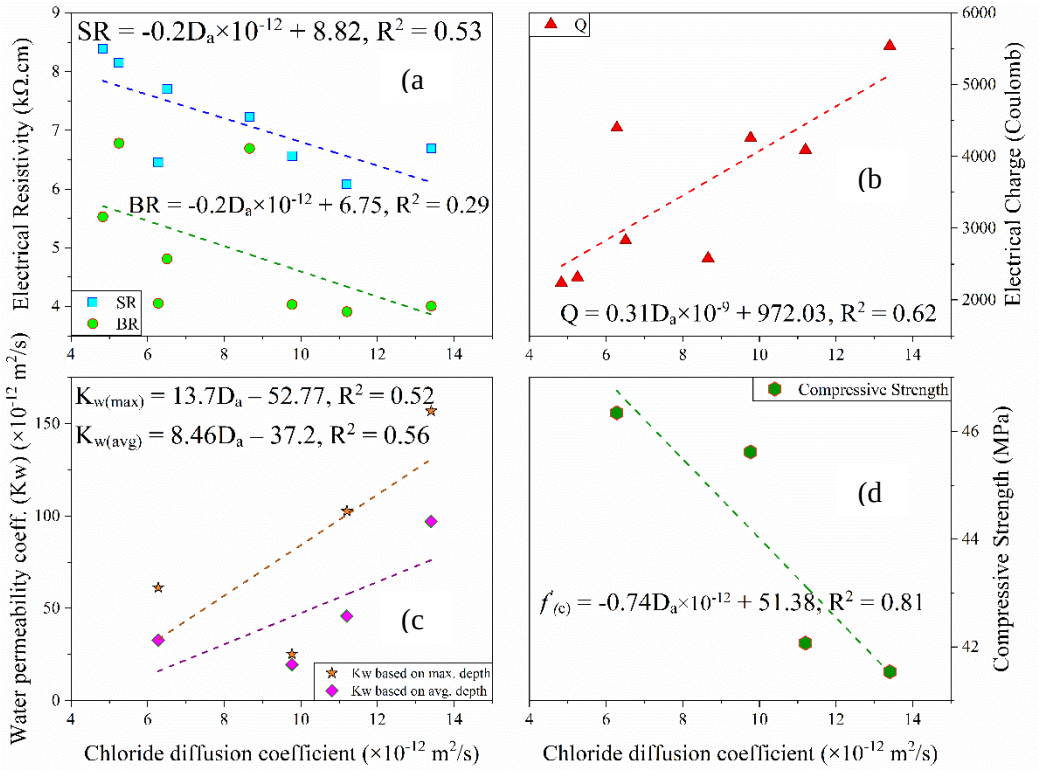

Fig. 12. Variation of apparent chloride diffusion coefficient with (a) ER, (b) WP, (c) RCP, and (d) strength of concrete.

3.6.6 Correlation between durability properties and compressive strength

Due to the mutual influence of pore structure on mechanical and durability properties, there is a great interest to relate transport properties and compressive strength of concrete. Hence, to investigate the interdependence between the properties of the concrete mixtures, values of compressive strength with certain durability parameters such as ER and *Q*, were compared. No significant linear relationship between the resistivity/RCP and compressive strength was found; however, it is noteworthy that the correlation coefficient of the correlation between water permeability and strength results is relatively

high. The relationships between physical and chemical effects of CA in improving concrete durability could play a vital role in performance-based design of concrete materials and structures. In addition, a relationship between compressive strength and chloride diffusion was established in this study [Fig. 12-(d)]. To sum up, all results collected from different test methods, Table 5 is presented for concretes with and without CA/PLC which included standardized penetration classification. Use of CA indicated better performance in improving water permeability and chloride diffusivity. According to concrete resistivity results, not much development was observed when using CA which opens up a need for further investigation of this parameter. As concrete ages, its durability properties also significantly improve as can be seen from Table 5.

Table5. Summary of conducted durability indicator test results.

Mix ID			**OPC**	**OPC-CA**	**PLC**	**PLC-CA**
Compressive strength (MPa)		28-day	41.54	46.35	42.07	45.62
Electrical resistivity (kΩ.cm)	SR (kΩ.cm)	28-day	6.69 (High)	6.45 (High)	6.08 (High)	6.57 (High)
		56-day	8.15 (High)	8.38 (High)	7.23 (High)	7.7 (High)
	BR (kΩ.cm)	28-day	4.01 (High)	4.06 (High)	3.91 (High)	4.03 (High)
		56-day	6.78 (Moderate)	5.53 (Moderate)	6.69 (Moderate)	4.81 (High)
Electrical charge (Coulombs)		28-day	5538 (High)	4399.25 (High)	4089.25 (High)	4257.75 (High)
		56-day	2314.75 (Moderate)	2238 (Moderate)	2578.75 (Moderate)	2827 (Moderate)
Water permeability coefficient ($\times 10^{-12}$ m^2/s)	Based on max. depth		156.92	61.2	102.71	25.2
	Based on avg. depth		97.08	32.81	45.73	19.57
Apparent chloride diffusion coefficient ($\times 10^{-12}$ m^2/s)		28-day	13.4 (Moderate)	6.28 (Low)	11.2 (Moderate)	9.77 (Low)
		56-day	5.25 (Low)	4.83 (very low)	8.66 (Low)	6.51 (Low)

3.7 Investigation of self-healing efficiency

The surface crack width (mm), measured initial flow, percent flow-reduction rate, and healing ratio (HR) of three cylinders for each mix are summarized in Table 6. From the analyzed data in Table 6, it is clear that the samples being compared had almost similar average surface crack width. The OPC samples had an average measured crack width of 0.244 mm as compared to 0.245 mm for OPC-CA, 0.251 mm for PLC, and 0.247 mm for PLC-CA. As expected, the higher the crack width, the higher the initial flow. The effect of healing was examined by calculating a HR parameter as follows (Equation 14) [58]:

$$Healing\ Ratio = 1 - \frac{Final\ Flow}{Initial\ Flow} = 1 - \frac{q_F}{q_0} > 0 \qquad \text{Equation 14}$$

where q_0 is the initial water flow (lit/5 min), measured after running self-healing apparatus; q_F is the final water flow (lit/5 min), measured after a healing period of 100 h. Presence of CA show slightly higher HR compared to control concretes; however, the average HR values were generally very close to each other.

Table 6. Measured crack width and intial flow.

Sample ID		Surface crack width (mm)				Real initial flow q_0 (lit/5 min)	Healing ratio
		Top	Bottom	Average			
OPC	I	0.226	0.290	0.258	0.2443	0.0696	0.991
	II	0.292	0.268	0.280		0.1891	0.938
	III	0.184	0.206	0.195		0.0248	0.941
OPC-CA	I	0.230	0.254	0.242	0.2453	0.0575	0.996
	II	0.332	0.275	0.304		0.1926	0.985
	III	0.176	0.205	0.191		0.0290	0.997
PLC	I	0.185	0.226	0.206	0.2510	0.0226	0.988
	II	0.325	0.25	0.288		0.1826	0.982
	III	0.244	0.273	0.259		0.0796	0.995
PLC-CA	I	0.203	0.263	0.233	0.2467	0.0915	0.975
	II	0.248	0.192	0.220		0.0378	0.990
	III	0.330	0.243	0.287		0.2294	0.992

The results of reduction in water flow and healing ratio over time is presented in Fig. 13. One can observe that the specimens experienced a rapid initial flow during the first day of exposure to water pressure; however, the flow reached a constant rate and a fairly steady curve within days. As can be seen, the flow through the specimens reduced over time, indicating "self-healing" of concrete. The addition of the crystalline admixtures yielded positive results with regards to self-healing as slope of flow rate line dropped significantly within few hours after testing for CA treated samples, not the case for control ones. It is hypothesized that the deposition of crystals into the crack which acts as membrane and hydrophilic nature of these admixtures can contribute to further fill the pores and create enough time for concrete to improve its natural healing process; thus, seal the cracks. By adding 3-4 % into the matrix, the enhancement of CA effectiveness under water pressure has been also confirmed by other studies [1,25,56-58], reporting 7-10% increase in the healing capability with respect to control samples, similar to those observed in this work. From this data, the time required for flow to reduce to a certain threshold value can be determined or the time required for completing

sealing of cracks can also be found. As seem from Fig. 13-(c) , with the increase of healing time, the HR ratio (especially for CA treated samples) were increased. Among all mixtures, OPC showed the lowest healing rate over time while CA group indicated ~90% healing within first 30 h of testing. A clear tendency of better healing rates can be seen when increasing the time and available water.

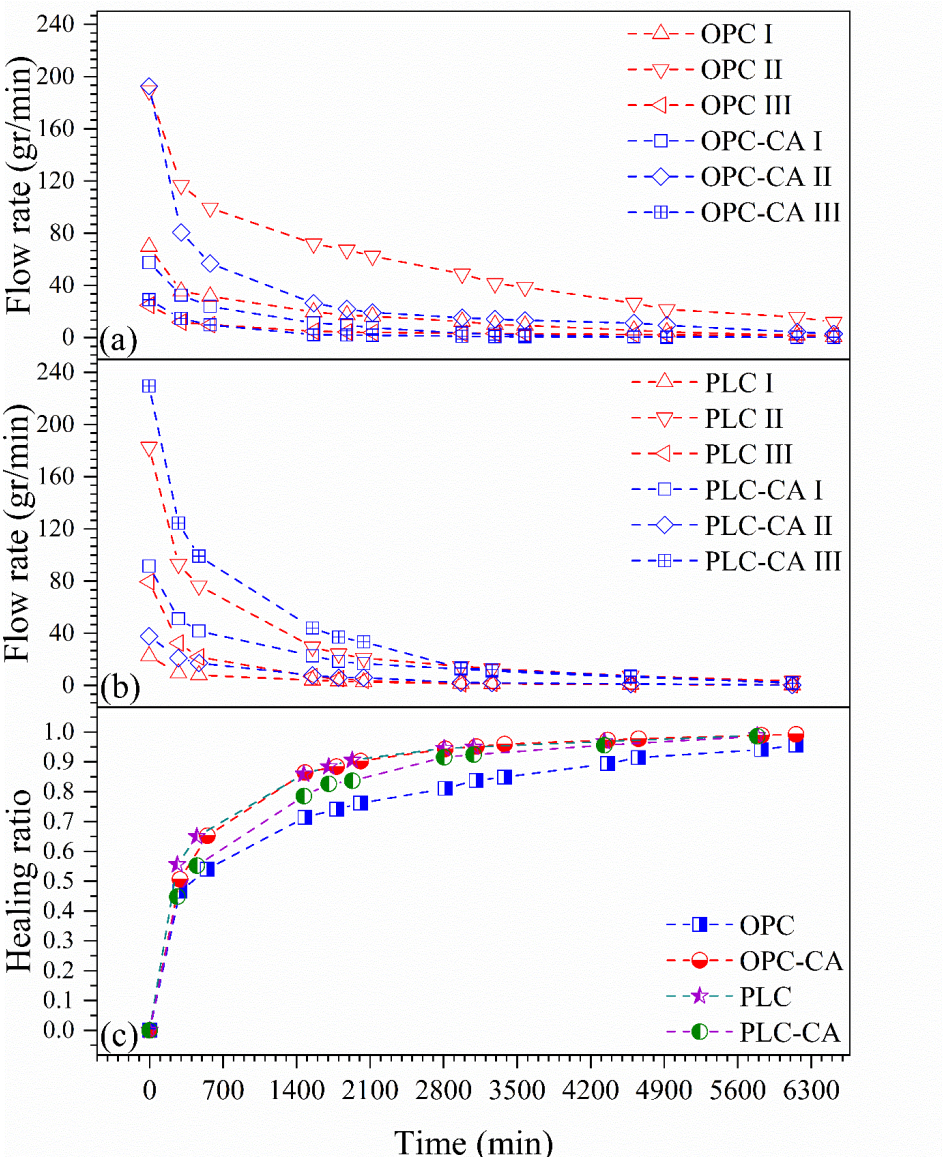

Fig. 13. Relationship between water flow and time for (a) OPC and OPC-CA specimens, (b) PLC and PLC-CA samples, (c) healing ratio vs. time for all mixtures.

Based on Poiseuille's law, Edvardsen proposed a model that determines the relation between the water flow passing through a crack and the crack width which is a third-order polynomial with only the cubic term [19]. The model is expressed in Equation 15:

$$q_o\left(\frac{liters}{h}\right) = 740 \times I \times CW_{avg}^3 \times k_t \qquad \text{Equation 15}$$

where q_o is the initial water leakage per meter visible crack length (lit/h); I is hydraulic gradient, m of water head/m; CW_{avg} is average crack width at the surface (mm); k_t is factor comprising different water temperature (k_t = 1 for water at 20°C with viscosity $\nu = \frac{\eta}{\rho} = 1.00$ mm^2/s). This expression can be adjusted to the parameters of this study by changing units and the crack length (considered 75 mm), resulting in the expression:

$$q_o\left(\frac{liters}{h}\right) = 740 \times \frac{1.5}{0.15} \times CW_{avg}^3 \times 1 \times 0.075 \qquad \text{Equation 16}$$

Fig. 14 shows the experimental values of initial water flow measured at beginning of self-healing test versus the corresponding initial average crack width of all specimens. The best fitting curve was set to be a cubic function as shown in Fig. 14. The results show that there is an acceptable correlation between q_0 and crack width with determination coefficient of 0.76. The obtained fitting curve from experimental results of water flow and averaged crack width fit reasonably well in the theoretical predictions given by Equation 16, illustrated also in Fig. 14. The lower experimental values might be due to the inclusion of CA which could help block water flow inside the crack or due to the difference in crack profile/structure inside the specimen. As self-healing could also be occurring inside the sample, not only on the surface crack, this correlation can only be utilized to compare the parameters of healing, rather than to draw an exact relationship between both parameters. An attempt was also made to use the minimum and maximum crack width instead of average values and find a correlation between these values and initial water flow. No affirmative trend was observed between these parameters. This finding is in agreement with the study of Roig-Flores et al. [57].

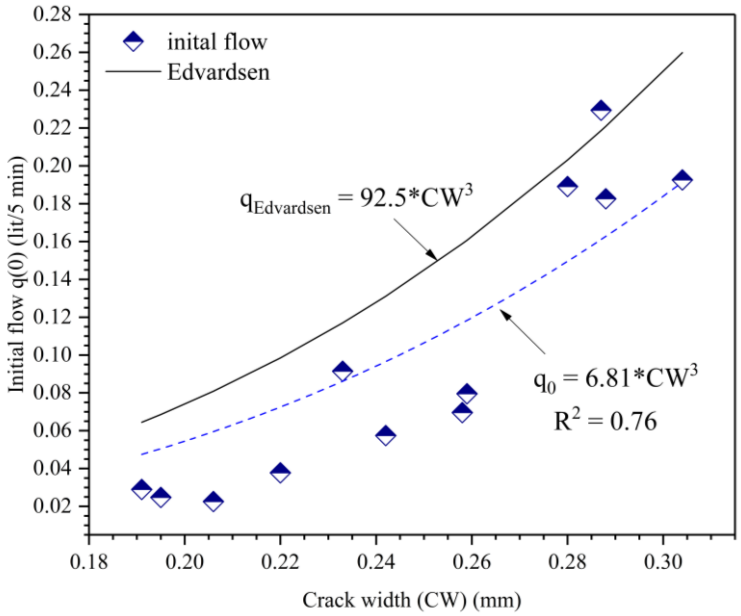

Fig. 14. Comparison between experimental and theoretical water flow and averaged crack width results.

4. Conclusions

In this study, the influence of the crystalline admixtures (CA) as permeability reducing admixtures on the durability and self-healing of concrete was investigated. In this paper, durability parameters including water penetration, chloride diffusivity, and electrical resistivity of concrete are investigated and correlated. The following conclusions can be drawn based on the results obtained in this study:

- Concretes treated with CA had almost 50% lower water penetration depth and thus lower permeability coefficient when compared to control mixes. When compared with OPC group, PLC concrete group indicated 20% and 37.5% lower water penetration depth for un- and CA-treated, respectively. Generally, the average water penetration depth appeared to be a better indicator to determine the water permeability coefficient than those obtained from maximum depth.
- The average cumulative charge, taken from RCP test to provide indirect information about concrete chloride diffusivity, was 5538 Coulombs for OPC, and was approximately 25%, 35%, and 30% higher for OPC-CA, PLC, and PLC-CA, respectively. This value was 2315 Coulombs for OPC at 56 days, roughly 5% higher than OPC-CA, and was 11% and 19% lower for PLC and PLC-CA mixtures, respectively. The difference in the total charge passed (coulombs) in RCP test between concrete mixtures with and without CA was inconsistent.
- Due to its simplicity, rapid-measurement, and low-cost associated with this non-destructive testing technique, concrete's electrical resistivity can be an alternative to the time-consuming permeability indicator test methods such as RCP or DIN 1048. Through this study, strong linear correlation was observed between SR and BR measurements, indicating the use of these resistivity test techniques interchangeably after considering an appropriate correction factor. The presence of CA did not reveal any significant effect on the surface or bulk electrical resistivity of concrete in comparison to the control mix.
- A nonlinear relationship between concrete SR (or BR) and its curing age was established, showing dependency of resistivity on sample's age. It was also hypothesized that either dosage of CA added to concrete was not sufficient to result in resistivity alteration and/or resistivity measurement method may not be a suitable technique to indirectly provide information about the CA's role in decreasing permeability. This is in contrast with results obtained from water penetration tests which showed significant improvement.
- The self-healing test results showed that addition of CA into mix led to slightly better rate of healing and full water-flow termination within the chosen test period when compared to control samples. PLC self-healing potential is reported for the first time in this work.
- According to the results of the ponding test, the use of CA helps in enhancing the resistance to chloride penetration. This improvement increases with increasing in concrete age.

Implementing Fick's second law, equations were proposed in this work to predict chloride content of CA-modified and control (OPC or PLC) specimens cured for 28 and 56 days.

5. Conflict of Interest

The authors declare that there is no conflict of interest regarding the publication of this paper.

6. Acknowledgment

The authors acknowledge financial support of National Sciences and Engineering Research Council (NSERC) of Canada for this project. The authors would also like to thank Kryton International for the engagement and material donation.

7. References

[1] L. Ferrara, V. Krelani, and F. Moretti, "On the use of crystalline admixtures in cement based construction materials: from porosity reducers to promoters of self healing," *Smart Mater. Struct.*, vol. 25, no. 8, p. 084002, Aug. 2016.

[2] A. El-Newihy, P. Azarsa, R. Gupta, and A. Biparva, "Effect of Polypropylene Fibers on Self-Healing and Dynamic Modulus of Elasticity Recovery of Fiber Reinforced Concrete," *Fibers*, vol. 6, no. 1, p. 9, Feb. 2018.

[3] W. Ramm and M. Biscoping, "Autogenous healing and reinforcement corrosion of water-penetrated separation cracks in reinforced concrete," *Nucl. Eng. Des.*, vol. 179, no. 2, pp. 191–200, Feb. 1998.

[4] N. Hearn and C. T. Morley, "Self-sealing property of concrete—Experimental evidence," *Mater. Struct.*, vol. 30, no. 7, pp. 404–411, Aug. 1997.

[5] Adam Neville, "Autogenous Healing—A Concrete Miracle?," *Concr. Int.*, vol. 24, no. 11, Nov. 2002.

[6] Mo Li and Victor C. Li, "Cracking and Healing of Engineered Cementitious Composites under Chloride Environment," *Mater. J.*, vol. 108, no. 3, May 2011.

[7] M. Şahmaran, S. B. Keskin, G. Ozerkan, and I. O. Yaman, "Self-healing of mechanically-loaded self consolidating concretes with high volumes of fly ash," *Cem. Concr. Compos.*, vol. 30, no. 10, pp. 872–879, Nov. 2008.

[8] Y. Yang, M. D. Lepech, E.-H. Yang, and V. C. Li, "Autogenous healing of engineered cementitious composites under wet–dry cycles," *Cem. Concr. Res.*, vol. 39, no. 5, pp. 382–390, May 2009.

[9] H.-W. Reinhardt and M. Jooss, "Permeability and self-healing of cracked concrete as a function of temperature and crack width," *Cem. Concr. Res.*, vol. 33, no. 7, pp. 981–985, Jul. 2003.

[10] S. Granger, A. Loukili, G. Pijaudier-Cabot, and G. Chanvillard, "Experimental characterization of the self-healing of cracks in an ultra high performance cementitious material: Mechanical tests and acoustic emission analysis," *Cem. Concr. Res.*, vol. 37, no. 4, pp. 519–527, Apr. 2007.

[11] W. Zamorowski, "The phenomenon of self-regeneration of concrete," *Int. J. Cem. Compos. Lightweight Concr.*, vol. 7, no. 3, pp. 199–201, Aug. 1985.

[12] N. Hearn, "Self-sealing, autogenous healing and continued hydration: What is the difference?," *Mater. Struct.*, vol. 31, no. 8, p. 563, Oct. 1998.

[13] S. Jacobsen and E. J. Sellevold, "Self healing of high strength concrete after deterioration by freeze/thaw," *Cem. Concr. Res.*, vol. 26, no. 1, pp. 55–62, Jan. 1996.

[14] C.-M. Aldea, W.-J. Song, J. S. Popovics, and S. P. Shah, "Extent of Healing of Cracked Normal Strength Concrete," *J. Mater. Civ. Eng.*, vol. 12, no. 1, pp. 92–96, Feb. 2000.

[15] M. L. Mustafa Sahmaran and Victor C. Li, "Transport Properties of Engineered Cementitious Composites under Chloride Exposure," *Mater. J.*, vol. 104, no. 6, Nov. 2007.

[16] S. Jacobsen, J. Marchand, and L. Boisvert, “Effect of cracking and healing on chloride transport in OPC concrete,” *Cem. Concr. Res.*, vol. 26, no. 6, pp. 869–881, Jun. 1996.
[17] D. Snoeck and N. De Belie, “Mechanical and self-healing properties of cementitious composites reinforced with flax and cottonised flax, and compared with polyvinyl alcohol fibres,” *Biosyst. Eng.*, vol. 111, no. 4, pp. 325–335, Apr. 2012.
[18] D. Homma, H. Mihashi, and T. Nishiwaki, “Self-Healing Capability of Fibre Reinforced Cementitious Composites,” *J. Adv. Concr. Technol.*, vol. 7, no. 2, pp. 217–228, 2009.
[19] Carola Edvardsen, “Water Permeability and Autogenous Healing of Cracks in Concrete,” *Mater. J.*, vol. 96, no. 4, Jul. 1999.
[20] V. C. Li and E. Herbert, “Robust Self-Healing Concrete for Sustainable Infrastructure,” *J. Adv. Concr. Technol.*, vol. 10, no. 6, pp. 207–218, 2012.
[21] S. R. White *et al.*, “Autonomic healing of polymer composites,” *Nature*, vol. 409, no. 6822, pp. 794–797, Feb. 2001.
[22] H. Mihashi, Y. Kaneko, T. Nishiwaki, and K. Otsuka, *Fundamental Study on Development of Intelligent Concrete Characterized by Self-Healing Capability for Strength*, vol. 11. 2000.
[23] B. Boh Podgornik and B. Sumiga, *Microencapsulation technology and its applications in building construction materials*, vol. 55. 2008.
[24] T.-H. Ahn and T. Kishi, “Crack Self-healing Behavior of Cementitious Composites Incorporating Various Mineral Admixtures,” *J. Adv. Concr. Technol.*, vol. 8, no. 2, pp. 171–186, 2010.
[25] K. Sisomphon, O. Copuroglu, and E. A. B. Koenders, “Self-healing of surface cracks in mortars with expansive additive and crystalline additive,” *Cem. Concr. Compos.*, vol. 34, no. 4, pp. 566–574, Apr. 2012.
[26] A. Jefferson, C. Joseph, R. Lark, B. Isaacs, S. Dunn, and B. Weager, “A new system for crack closure of cementitious materials using shrinkable polymers,” *Cem. Concr. Res.*, vol. 40, no. 5, pp. 795–801, May 2010.
[27] G. Song, N. Ma, and H.-N. Li, “Applications of shape memory alloys in civil structures,” *Eng. Struct.*, vol. 28, no. 9, pp. 1266–1274, Jul. 2006.
[28] V. Wiktor and H. M. Jonkers, “Quantification of crack-healing in novel bacteria-based self-healing concrete,” *Cem. Concr. Compos.*, vol. 33, no. 7, pp. 763–770, Aug. 2011.
[29] J. Y. Wang, D. Snoeck, S. Van Vlierberghe, W. Verstraete, and N. De Belie, “Application of hydrogel encapsulated carbonate precipitating bacteria for approaching a realistic self-healing in concrete,” *Constr. Build. Mater.*, vol. 68, pp. 110–119, Oct. 2014.
[30] J. Wang, K. Van Tittelboom, N. De Belie, and W. Verstraete, “Use of silica gel or polyurethane immobilized bacteria for self-healing concrete,” *Constr. Build. Mater.*, vol. 26, no. 1, pp. 532–540, Jan. 2012.
[31] K. Van Tittelboom, N. De Belie, W. De Muynck, and W. Verstraete, “Use of bacteria to repair cracks in concrete,” *Cem. Concr. Res.*, vol. 40, no. 1, pp. 157–166, Jan. 2010.
[32] Carolyn Dry, “Matrix cracking repair and filling using active and passive modes for smart timed release of chemicals from fibers into cement matrices,” *Smart Mater. Struct.*, vol. 3, no. 2, p. 118, 1994.
[33] C. Dry, “Procedures developed for self-repair of polymer matrix composite materials,” *Compos. Struct.*, vol. 35, no. 3, pp. 263–269, Jul. 1996.
[34] V. C. Li, Y. M. Lim, and Y.-W. Chan, “Feasibility study of a passive smart self-healing cementitious composite,” *Compos. Part B Eng.*, vol. 29, no. 6, pp. 819–827, Nov. 1998.
[35] C. Joseph, A. D. Jefferson, B. Isaacs, R. Lark, and D. Gardner, “Experimental investigation of adhesive-based self-healing of cementitious materials,” *Mag. Concr. Res.*, vol. 62, no. 11, pp. 831–843, Nov. 2010.
[36] T. D. P. Thao, T. J. S. Johnson, Q. S. Tong, and P. S. Dai, “Implementation of self-healing in concrete – Proof of concept,” *IES J. Part Civ. Struct. Eng.*, vol. 2, no. 2, pp. 116–125, May 2009.
[37] T. Nishiwaki, H. Mihashi, B.-K. Jang, and K. Miura, “Development of Self-Healing System for Concrete with Selective Heating around Crack,” *J. Adv. Concr. Technol.*, vol. 4, no. 2, pp. 267–275, 2006.

[38] J. W. C. Pang and I. P. Bond, “A hollow fibre reinforced polymer composite encompassing self-healing and enhanced damage visibility,” *Compos. Sci. Technol.*, vol. 65, no. 11, pp. 1791–1799, Sep. 2005.
[39] S. . Bleay, C. . Loader, V. . Hawyes, L. Humberstone, and P. . Curtis, “A smart repair system for polymer matrix composites,” *Compos. Part Appl. Sci. Manuf.*, vol. 32, no. 12, pp. 1767–1776, Dec. 2001.
[40] M Motuku and U K Vaidya and G M Janowski, “Parametric studies on self-repairing approaches for resin infused composites subjected to low velocity impact,” *Smart Mater. Struct.*, vol. 8, no. 5, p. 623, 1999.
[41] Carolyn Dry and William McMillan, “Three-part methylmethacrylate adhesive system as an internal delivery system for smart responsive concrete,” *Smart Mater. Struct.*, vol. 5, no. 3, p. 297, 1996.
[42] S. Qian, J. Zhou, M. R. de Rooij, E. Schlangen, G. Ye, and K. van Breugel, “Self-healing behavior of strain hardening cementitious composites incorporating local waste materials,” *Cem. Concr. Compos.*, vol. 31, no. 9, pp. 613–621, Oct. 2009.
[43] H.-S. S. Li-Li Kan Aaron R. Sakulich, and Victor C. Li, “Self-Healing Characterization of Engineered Cementitious Composite Materials,” *Mater. J.*, vol. 107, no. 6, Nov. 2010.
[44] E. Herbert and V. Li, “Self-Healing of Microcracks in Engineered Cementitious Composites (ECC) Under a Natural Environment,” *Materials*, vol. 6, no. 7, pp. 2831–2845, Jul. 2013.
[45] M. S. Erdogan Ozbay Mohamed Lachemi, and Hasan Erhan Yucel, “Self-Healing of Microcracks in High-Volume Fly-Ash- Incorporated Engineered Cementitious Composites,” *Mater. J.*, vol. 110, no. 1, Jan. 2013.
[46] M. Sahmaran, G. Yildirim, and T. K. Erdem, “Self-healing capability of cementitious composites incorporating different supplementary cementitious materials,” *Cem. Concr. Compos.*, vol. 35, no. 1, pp. 89–101, Jan. 2013.
[47] M. Şahmaran, G. Yildirim, E. Ozbay, K. Ahmed, and M. Lachemi, “Self-healing ability of cementitious composites: effect of addition of pre-soaked expanded perlite,” *Mag. Concr. Res.*, vol. 66, no. 8, pp. 409–419, Apr. 2014.
[48] G. Yildirim, M. Sahmaran, and H. U. Ahmed, “Influence of Hydrated Lime Addition on the Self-Healing Capability of High-Volume Fly Ash Incorporated Cementitious Composites,” *J. Mater. Civ. Eng.*, vol. 27, no. 6, p. 04014187, Jun. 2015.
[49] G. Yildirim, A. Alyousif, M. Şahmaran, and M. Lachemi, "Assessing the self-healing capability of cementitious composites under increasing sustained loading," *J Advances in Cement Research*, 27(10), 581-592, 2015.
[50] G. Yıldırım, A.H. Khiavi, S. Yeşilmen, and M. Şahmaran, "Self-healing performance of aged cementitious composites," *Cement and Concrete Composites*, 87, 172-186, 2018.
[51] M. Sahmaran, G. Yıldırım, G.H. Aras, S.B. Keskin, O.K. Keskin, and M Lachemi, "Self-Healing of Cementitious Composites to Reduce High CO2 Emissions," *Materials Journal*, 114(01), 93-104, 2017.
[52] ACI Committee 212, *ACI 212. 3R-16 Report on Chemical Admixtures for Concrete*. American Concrete Institute, 2016.
[53] D. Jaroenratanapirom and R. Sahamitmongkol, “Effects of different mineral additives and cracking ages on self-healing performance of mortar,” presented at the Annual Concrete Conference 6, 2011.
[54] D. Jaroenratanapirom and R. Sahamitmongkol, “Self-Crack Closing Ability of Mortar with Different Additives,” *J. Met. Mater. Miner.*, vol. 21, pp. 9–17, 2011.
[55] K. Sisomphon, O. Copuroglu, and E. A. B. Koenders, “Effect of exposure conditions on self healing behavior of strain hardening cementitious composites incorporating various cementitious materials,” *Constr. Build. Mater.*, vol. 42, pp. 217–224, May 2013.
[56] L. Ferrara, V. Krelani, and M. Carsana, “A ‘fracture testing’ based approach to assess crack healing of concrete with and without crystalline admixtures,” *Constr. Build. Mater.*, vol. 68, pp. 535–551, Oct. 2014.
[57] M. Roig-Flores, S. Moscato, P. Serna, and L. Ferrara, “Self-healing capability of concrete with crystalline admixtures in different environments,” *Constr. Build. Mater.*, vol. 86, pp. 1–11, Jul. 2015.

[58] M. Roig-Flores, F. Pirritano, P. Serna, and L. Ferrara, “Effect of crystalline admixtures on the self-healing capability of early-age concrete studied by means of permeability and crack closing tests,” *Constr. Build. Mater.*, vol. 114, pp. 447–457, Jul. 2016.
[59] British Standards Institution, *Testing hardened concrete. Part 8, Part 8,*. London: BSI, 2009.
[60] R. Gupta and A. Biparva, “Innovative Test Technique to Evaluate ‘Self-Sealing’ of Concrete,” *J. Test. Eval.*, vol. 43, no. 5, p. 20130285, Sep. 2015.
[61] ASTM C1202-12, “Standard Test Method for Electrical Indication of Concrete’s Ability to Resist Chloride Ion Penetration,” *ASTM Int.*, 2012.
[62] AASHTO TP 95, “Method of Test for Surface Resistivity Indication of Concrete’s Ability to Resist Chloride Ion Penetration,” *Am. Assoc. State Highw. Transp. Off.*, 2011.
[63] ASTM C1556, “Standard Test Method for Determining the Apparent Chloride Diffusion Coefficient of Cementitious Mixtures by Bulk Diffusion.” ASTM International, 2016.
[64] DIN 1048, “Testing Concrete: Testing of Hardened Concrete (Specimens prepared in mould).” Deutscher Ausschuß für Stahlbeton of the Normenausschuß Bauwesen, 1991.
[65] CSA A23.1-14, “Standard for concrete materials and methods of concrete construction.” Canadian Standard Association (CSA), 2014.
[66] ASTM C192 / C192M-15, “Standard Practice for making and Curing Concrete Test Specimens in the Laboratory.” ASTM International, 2015.
[67] ASTM C143 / C143M-15a, “Standard Test Method for Slump of Hydraulic-Cement Concrete.” ASTM International, 2015.
[68] ASTM C231 / C231M-14, “Standard Test Method for Air Content of Freshly Mixed Concrete by the Pressure Method.” ASTM International, 2014.
[69] ASTM C138 / C138M-17a, “Standard Test Method for Density (Unit Weight), Yield, and Air Content (Gravimetric) of Concrete.” ASTM International, 2017.
[70] ASTM C1064 / C1064M-12, “Standard Test Method for Temperature of Freshly Mixed Hydraulic-Cement Concrete.” ASTM International, 2012.
[71] ASTM C39 / C39M-15a, “Standard Test Method for Compressive Strength of Cylindrical Concrete Specimens.” ASTM International, 2015.
[72] G. Yıldırım, G.H. Aras, Q.S. Banyhussan, M. Şahmaran, and M. Lachemi, "Estimating the self-healing capability of cementitious composites through non-destructive electrical-based monitoring,"*Ndt & E International*, 76, 26-37, 2015.
[73] A. Al-Dahawi, M.H. Sarwary, O. Öztürk, G. Yıldırım, A. Akın, M. Şahmaran, and M. Lachemi, "Electrical percolation threshold of cementitious composites possessing self-sensing functionality incorporating different carbon-based materials," *Smart Materials and Structures*, 25(10), 105005, 2016.
[74] M. Ibrahim and M. Issa, “Evaluation of chloride and water penetration in concrete with cement containing limestone and IPA,” *Constr. Build. Mater.*, vol. 129, pp. 278–288, Dec. 2016.
[75] P. A. . Basheer, P. R. . Gilleece, A. . Long, and W. . Mc Carter, “Monitoring electrical resistance of concretes containing alternative cementitious materials to assess their resistance to chloride penetration,” *Cem. Concr. Compos.*, vol. 24, no. 5, pp. 437–449, Oct. 2002.
[76] P. Ghosh and Q. Tran, “Correlation Between Bulk and Surface Resistivity of Concrete,” *Int. J. Concr. Struct. Mater.*, vol. 9, no. 1, pp. 119–132, Mar. 2015.
[77] P. Ghosh and Q. Tran, “Influence of parameters on surface resistivity of concrete,” *Cem. Concr. Compos.*, vol. 62, pp. 134–145, Sep. 2015.
[78] K. M. Smith, A. J. Schokker, and P. J. Tikalsky, “Performance of Supplementary Cementitious Materials in Concrete Resistivity and Corrosion Monitoring Evaluations,” *ACI Mater. J.*, vol. 101, no. 5, Sep. 2004.
[79] P. Azarsa and R. Gupta, “Electrical Resistivity of Concrete for Durability Evaluation: A Review,” *Adv. Mater. Sci. Eng.*, vol. 2017, pp. 1–30, 2017.
[80] H. Layssi, P. Ghods, A. R. Alizadeh, and M. Salehi, “Electrical Resistivity of Concrete,” *Concrete International*, pp. 41–46, May-2015.
[81] E. G. Moffatt, M. D. A. Thomas, and A. Fahim, “Performance of high-volume fly ash concrete in marine environment,” *Cem. Concr. Res.*, vol. 102, pp. 127–135, Dec. 2017.
[82] M. M. Khotbehsara, B. M. Miyandehi, F. Naseri, T. Ozbakkaloglu, F. Jafari, and E. Mohseni, “Effect of SnO 2 , ZrO 2 , and CaCO 3 nanoparticles on water transport and durability

properties of self-compacting mortar containing fly ash: Experimental observations and ANFIS predictions," *Constr. Build. Mater.*, vol. 158, pp. 823–834, Jan. 2018.
[83] S. A. Bernal, R. Mejía de Gutiérrez, and J. L. Provis, "Engineering and durability properties of concretes based on alkali-activated granulated blast furnace slag/metakaolin blends," *Constr. Build. Mater.*, vol. 33, pp. 99–108, Aug. 2012.
[84] A. A. Ramezanianpour, A. Pilvar, M. Mahdikhani, and F. Moodi, "Practical evaluation of relationship between concrete resistivity, water penetration, rapid chloride penetration and compressive strength," *Constr. Build. Mater.*, vol. 25, no. 5, pp. 2472–2479, May 2011.
[85] A. A. Ramezanianpour and H. Bahrami Jovein, "Influence of metakaolin as supplementary cementing material on strength and durability of concretes," *Constr. Build. Mater.*, vol. 30, pp. 470–479, May 2012.
[86] M. Khoshroo, A. A. Shirzadi Javid, and A. Katebi, "Effects of micro-nano bubble water and binary mineral admixtures on the mechanical and durability properties of concrete," *Constr. Build. Mater.*, vol. 164, pp. 371–385, Mar. 2018.
[87] R. J. Thomas, E. Ariyachandra, D. Lezama, and S. Peethamparan, "Comparison of chloride permeability methods for Alkali-Activated concrete," *Constr. Build. Mater.*, vol. 165, pp. 104–111, Mar. 2018.
[88] Min-Hong Zhang and Odd E. Gjorv, "Permeability of High-Strength Lightweight Concrete," *Mater. J.*, vol. 88, no. 5, Sep. 1991.
[89] P. K. Mehta and P. J. M. Monteiro, *Concrete: microstructure, properties, and materials*, 3rd ed. New York: McGraw-Hill, 2006.
[90] S. E. Hedegaard and T. C. Hansen, "Water permeability of fly ash concretes," *Mater. Struct.*, vol. 25, no. 7, pp. 381–387, Aug. 1992.
[91] J. Zhang and Z. Lounis, "Sensitivity analysis of simplified diffusion-based corrosion initiation model of concrete structures exposed to chlorides," *Cem. Concr. Res.*, vol. 36, no. 7, pp. 1312–1323, Jul. 2006.
[92] A. da Costa, M. Fenaux, J. Fernández, E. Sánchez, and A. Moragues, "Modelling of chloride penetration into non-saturated concrete: Case study application for real marine offshore structures," *Constr. Build. Mater.*, vol. 43, pp. 217–224, Jun. 2013.
[93] A. Neville, "Chloride attack of reinforced concrete: an overview," *Mater. Struct.*, vol. 28, no. 2, p. 63, Mar. 1995.
[94] A. Keulen, Q. L. Yu, S. Zhang, and S. Grünewald, "Effect of admixture on the pore structure refinement and enhanced performance of alkali-activated fly ash-slag concrete," *Constr. Build. Mater.*, vol. 162, pp. 27–36, Feb. 2018.